Synthesis, Characterization, and Bromine Substitution by 4,4′-Di(5-nonyl)-2,2′-bipyridine in Cu^{II}(4,4′-di(5-nonyl)-2,2′-bipyridine)Br_2

Tomislav Pintauer,[†] Jian Qiu,[†] Guido Kickelbick,[‡] and Krzysztof Matyjaszewski*,[†]

Center for Macromolecular Engineering, Carnegie Mellon University, 4400 Fifth Avenue, Pittsburgh, Pennsylvania 15213, and Institut für Anorganische Chemie, Techniche Universität Wien, Getreidemarkt 9/153, 1060 Wien, Austria

Received January 8, 2001

The crystal structure of a novel compound Cu^{II}(dNbpy)Br_2 (dNbpy = 4,4′-di(5-nonyl)-2,2′-bipyridine), which is used in the reverse atom transfer radical polymerization, is reported. Cu^{II}(dNbpy)Br_2 crystallizes in the triclinic *P*1 space group with $a = 12.5283(11)$ Å, $b = 15.0256(14)$ Å, $c = 17.7900(16)$ Å, $\alpha = 90.350(2)°$, $\beta = 99.360(2)°$, $\gamma = 107.937(2)°$, and $Z = 2$. The Cu^{II} center in the complex has a distorted square planar geometry and is coordinated by two nitrogen atoms of a single dNbpy ligand (Cu−N = 2.011(7) and 2.022(7) Å) and two bromine atoms (Cu−Br = 2.3621(14) and 2.3567(13) Å). The similarity of the absorption spectra in the solid state and in solution suggested that the geometry of the complex remained unchanged upon dissolution. In the presence of dNbpy, Cu^{II}(dNbpy)Br_2 undergoes Br substitution to form ionic $[Cu^{II}(dNbpy)_2Br]^+[Br]^-$. $\Delta H°$ and $\Delta S°$ values for this equilibrium were negative and dependent on the polarity of the medium. It was found that, under the typical polymerization conditions ($T \geq 90$ °C and the total copper concentration in the range 1.0×10^{-2}−1.0×10^{-1} M), $Cu^{II}Br_2$ and 2 equiv of dNbpy will predominantly form the neutral Cu^{II}(dNbpy)Br_2 complex. In a polar medium under the same conditions, $[Cu^{II}(dNbpy)_2Br]^+[Br]^-$ is preferred.

Introduction

Since the discovery in 1995, atom transfer radical polymerization (ATRP) has experienced a substantial progress and has become one of the most powerful tools for obtaining well-defined polymers by radical means.[1−4] The catalytic cycle in ATRP involves reversible switching between two oxidation states of a transition metal complex.[5,6] Shown in Scheme 1 is the proposed mechanism for a typical polymerization system using a copper(I) halide/2,2′-bipyridine (bpy) derivative as the catalyst.[7] Homolytic cleavage of the alkyl halide bond (R−X) by the Cu^I complex generates an alkyl radical, R•, and the corresponding Cu^{II} complex. The radical R• can propagate, with a propagation rate constant k_p, by being added across the double bond of a vinyl monomer, terminate by either coupling or disproportionation (k_t), or reversibly deactivate by the Cu^{II} complex (k_d). Since the equilibrium is strongly shifted toward the dormant species ($k_a \ll k_d$), radical termination is suppressed. As a result of this persistent radical effect,[8,9] polymers with predictable molecular weights, narrow molecular weight distributions, and high functionalities can be synthesized.[10]

Scheme 1. Proposed Mechanism for ATRP

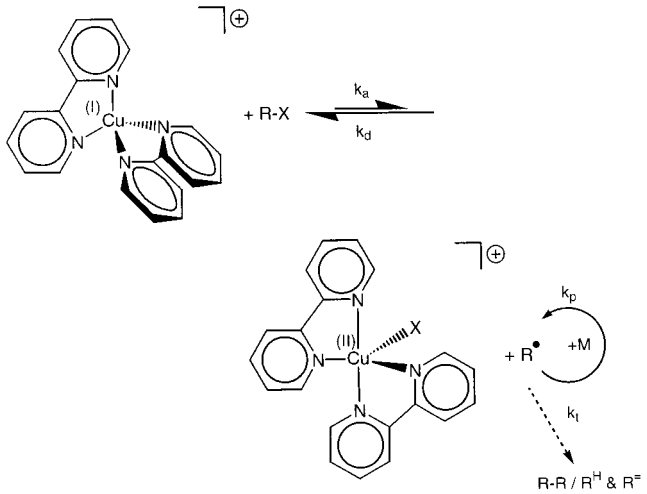

Another way to approach this atom transfer equilibrium is to start from a conventional radical initiator, such as azobis(isobutyronitrile) or benzoyl peroxide, and a Cu^{II} complex; the Cu^I complex and the alkyl halide are generated *in situ*. This process is called reverse ATRP.[11−13]

[†] Carnegie Mellon University.
[‡] Techniche Universität Wien.

(1) Kato, M.; Kamigaito, M.; Sawamoto, M.; Higashimura, T. *Macromolecules* **1995**, *28*, 1721−1723.
(2) Wang, J.-S.; Matyjaszewski, K. *J. Am. Chem. Soc.* **1995**, *117*, 5614−5615.
(3) *Controlled Radical Polymerization*; Matyjaszewski, K., Ed.; ACS Symposium Series 685; American Chemical Society: Washington, DC, 1998.
(4) *Controlled/Living Radical Polymerization: Progress in ATRP, NMP and RAFT*; Matyjaszewski, K., Ed.; ACS Symposium Series 768; American Chemical Society: Washington, DC, 2000.
(5) Matyjaszewski, K. *Chem. Eur. J.* **1999**, *5*, 3095−3102.
(6) Patten, T. E.; Matyjaszewski, K. *Acc. Chem. Res.* **1999**, *32*, 895−903.
(7) Matyjaszewski, K.; Patten, T. E.; Xia, J. *J. Am. Chem. Soc.* **1997**, *119*, 674−680.
(8) Fischer, H. *Macromolecules* **1997**, *30*, 5666−5672.
(9) Fischer, H. *J. Polym. Sci., Part A: Polym. Chem.* **1999**, *37*, 1885−1901.
(10) Patten, T. E.; Matyjaszewski, K. *Adv. Mater.* **1998**, *10*, 901−915.
(11) Wang, J.-S.; Matyjaszewski, K. *Macromolecules* **1995**, *28*, 7572−7573.
(12) Xia, J.; Matyjaszewski, K. *Macromolecules* **1997**, *30*, 7692−7696.
(13) Xia, J.; Matyjaszewski, K. *Macromolecules* **1999**, *32*, 5199−5202.

10.1021/ic0100267 CCC: $20.00
Published on Web 05/10/2001

The study of the structures of the Cu^{I} and Cu^{II} complexes involved in both conventional and reverse ATRP is essential for further understanding of this catalytic process. In conjunction with the chemistry and the dynamics associated with the atom transfer step between copper centers, they can provide much needed information about how to extend polymerization control to even higher molecular weight polymers, develop more active catalysts that can be used in smaller concentrations, and polymerize in a controlled fashion other monomers such as vinyl esters and dienes.

In this paper, we report the solid-state X-ray structure of a novel compound, $Cu^{II}(dNbpy)Br_2$ (dNbpy = 4,4′-di(5-nonyl)-2,2′-bipyridine). This complex, although not previously isolated, is used in our laboratories as the catalyst for reverse ATRP. Furthermore, thermodynamic parameters for the substitution of Br by dNbpy ligand in $Cu^{II}(dNbpy)Br_2$ were determined in various solvents including the monomers typically polymerizable by ATRP.

Experimental Section

$Cu^{II}Br_2$ (99.999%, Aldrich), $Cu^{II}(CF_3SO_3)_2$ (99%, Aldrich), and all solvents were used as received. dNbpy was prepared according to the literature procedure.[14] $[Cu^{II}(dNbpy)_2Br][Y]$ (Y = Br^-, PF_6^-, and $CF_3SO_3^-$) was prepared in CH_3CN according to the procedures for $[Cu^{II}(bpy)_2Br][Br]$,[15] $[Cu^{II}(bpy)_2Br][PF_6]$,[16] and $[Cu^{II}(bpy)_2Br][CF_3SO_3]$,[17] except that dNbpy was used instead of bpy ligand. The spectroscopic measurements were performed on a UV/VIS/NIR spectrometer (Lambda 900, Perkin-Elmer), using either a quartz UV cell joined to a Schlenk flask or a well-sealed test tube with a UV probe inserted (used when temperature adjustment was necessary). The UV probe was connected to the spectrometer via an optical fiber. The temperature adjustment was accomplished by using either a thermostated oil bath or a H_2O/ice mixture. Conductivity measurements were performed on an Amel conductivity meter equipped with a glass electrode. Conductivity was measured over a time interval of 10−15 min, and the average values were reported. All experiments were performed at room temperature using initial concentrations of $Cu^{II}(dNbpy)Br_2$ in the range of $1.0-3.0 \times 10^{-3}$ mol L^{-1}. Elemental analysis for H, C, and N were performed by Chemisar Laboratories Inc., Guelph, Ontario, Canada.

Synthesis of $Cu^{II}(dNbpy)Br_2$. $Cu^{II}Br_2$ (0.130 g, 5.78×10^{-4} mol) was dissolved in 15 mL of acetonitrile, and 0.236 g (5.78×10^{-4} mol) of dNbpy was added. The mixture was heated until it was homogeneous (dark purple). The solution was then cooled at −15 °C for 10 h. The dark purple crystals were filtered and dried under vacuum to yield 0.300 g (82% yield) of $Cu^{II}(dNbpy)Br_2$. The product was recrystallized from acetonitrile. Anal. Calcd for $Cu^{II}(C_{28}H_{44}N_2)Br_2$: C, 53.21; H, 7.02; N, 4.43. Found: C, 52.99; H, 7.34; N, 4.33.

X-ray Structure Analysis. The crystal structure data and experimental details are given in Table 1. The X-ray data were collected at room temperature on a Siemens SMART CCD area detector diffractometer using graphite monochromated Mo Kα radiation (λ = 0.710 73 Å), a nominal crystal-to-detector distance of 4.40 cm, and 0.3° ω scans frames. Corrections for Lorentz polarization effects and an empirical absorption correction with the program SADABS were applied.[18] The structures were solved by the Patterson method (SHELXS86) and were refined by the full-matrix least-squares method based on F^2 (SHELXL93). All non-hydrogen atoms were refined anisotropically, and the hydrogens were included in idealized positions.

(14) Hadda, T. B.; Bozec, H. L. *Polyhedron* **1988**, *7*, 575−577.
(15) Khan, M. A.; Tuck, D. G. *Acta Crystallogr., Sect. B*: *Struct. Sci.* **1981**, *B37*, 1409−1412.
(16) Crutchley, R. J.; Hynes, R.; Gabe, E. J. *Inorg. Chem.* **1990**, *29*, 4921−4928.
(17) O'Sullivan, C.; Murphy, G.; Murphy, B.; Hathaway, B. *J. Chem. Soc., Dalton Trans.* **1999**, *11*, 1835−1844.
(18) Sheldrick, G. *SADABS, Program for Siemens Area Detector Absorption Correction*; Institut fur Anorganische Chemie, Universitat Gottingen: Gottingen, Germany, 1996.

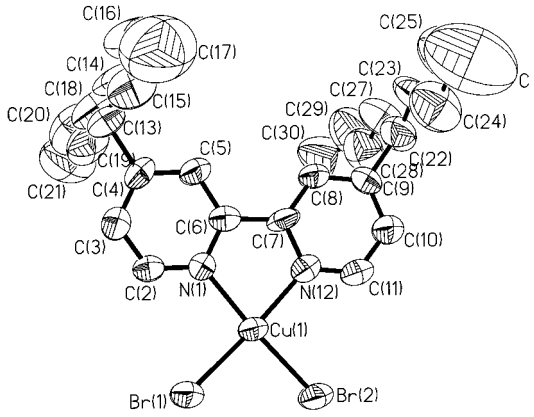

Figure 1. ORTEP drawing of $Cu^{II}(dNbpy)Br_2$ with 40% probability ellipsoids. Hydrogen atoms have been removed for clarity.

Table 1. Crystal Data and Structure Refinement for $Cu^{II}(dNbpy)Br_2$

empirical formula	$C_{28}H_{44}Br_2CuN_2$
fw	632.00
crystal system	triclinic
space group	$P\bar{1}$
unit cell dimensions (Å, deg)	a = 12.5283(11), α = 90.350(2)
	b = 15.0256(14), β = 99.360(2)
	c = 17.7900(16), γ = 107.937(2)
V (Å^3)	3138.1(5)
Z	2
ρ_{calcd} (g cm^{-3})	1.336
μ (mm^{-1})	3.259
F(000)	1296
crystal size (mm)	0.20 × 0.14 × 0.06
θ range for data collection (deg)	1.16−20.82
limiting indices	$-12 \le h \le 12$
	$-15 \le k \le 15$
	$-17 \le l \le 17$
reflns collected/unique	21 621/6562 [R(int) = 0.0798]
completeness to θ = 20.82	100.0%
max and min transmission	0.8285, 0.5618
data/restraints/params	6562/0/604
GOF on F^2	1.012
final R indices ($I > 2\sigma(I)$)	R1 = 0.0581
	wR2 = 0.1373
R indices (all data)	R1 = 0.1049
	wR2 = 0.1663
extinction coeff	0.0001(2)
largest diff peak and hole (e Å^{-3})	0.491, −0.515

Table 2. Selected Bond Distances (Å) and Angles (deg) for $Cu^{II}(dNbpy)Br_2$[a]

Distances			
Cu(1)−Br(1)	2.3621(14)	Cu(1)−Br(2)	2.3567(13)
Cu(1)−N(1)	2.011(7)	Cu(1)−N(12)	2.022(7)
Angles			
Br(1)−Cu(1)−Br(2)	91.74(5)	N(1)−Cu(1)−N(12)	80.4(3)
Br(1)−Cu(1)−N(1)	94.5(2)	Br(1)−Cu(1)−N(12)	169.9(2)
Br(2)−Cu(1)−N(1)	170.8(2)	Br(2)−Cu(1)−N(12)	94.5(2)

[a] Symmetry operations used to generate equivalent atoms: $-x, -y, -z$.

Results and Discussion

Crystal Structure of $Cu^{II}(dNbpy)Br_2$. In Figure 1 is shown the ORTEP plot of the $Cu^{II}(dNbpy)Br_2$ complex. Selected bond distances and angles are given in Table 2. The copper(II) center has a distorted square planar geometry and is coordinated by the two nitrogen atoms of a single dNbpy ligand and two bromine atoms. This square planar motif has been observed in the crystal structure of a closely related compound, $Cu^{II}(bpy)Br_2$.[19,20] The Cu−N and Cu−Br bond lengths in $Cu^{II}(dNbpy)$-

Table 3. Electronic Absorption Data (Vis/NIR) for $Cu^{II}Br_2$ Complexes with dNbpy

complex	solvent	λ_{max}/nm (ϵ^a/L mol^{-1} cm^{-1})		
Cu^{II}(dNbpy)Br_2	CH_3CN		736(242)	493(900)
	methyl acrylate		721(232)	512(899)
	methyl methacrylate		695(231)	517(882)
	butyl acrylate		700(249)	521(930)
	styrene		735sh(240)	525(900)
	toluene		730sh(230)	530(890)
$[Cu^{II}(dNbpy)_2Br]^+[Br]^-$	CH_3CN	933sh(230)	750(350)	
	MeOH	930sh(221)	753(356)	
$[Cu^{II}(dNbpy)_2Br]^+[PF_6]^-$	CH_3CN	950sh(175)	745(332)	
	MeOH	922sh(190)	744(352)	
	toluene	1000sh(160)	745(320)	
$[Cu^{II}(dNbpy)_2Br]^+[CF_3SO_3]^-$	CH_3CN	950sh(178)	743(340)	
	MeOH	950sh(180)	743(336)	
	toluene	970sh(180)	750(330)	

[a] Extinction coefficient calculated based on total Cu^{II} concentration; sh, shoulder of an absorption band.

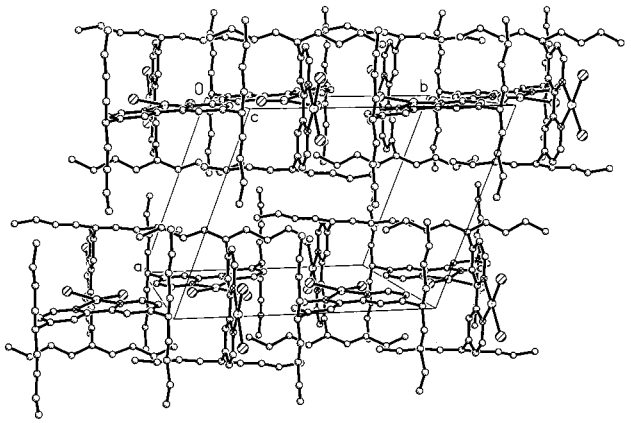

Figure 2. Crystal structure of Cu^{II}(dNbpy)Br_2 viewed along the *c*-axis.

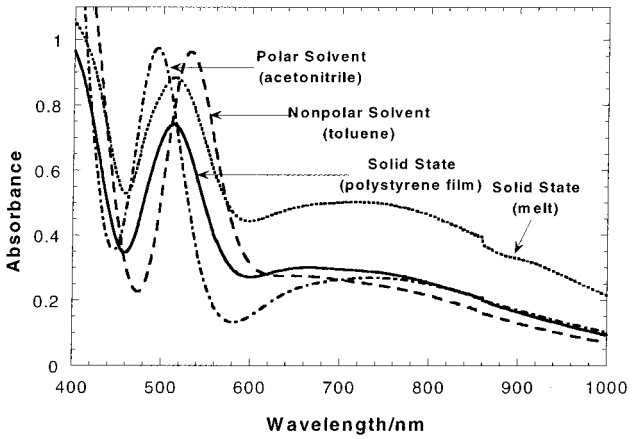

Figure 3. Absorption spectra (Vis/NIR) of Cu^{II}(dNbpy)Br_2.

Br_2 (Cu−N = 2.011(7), 2.022(7) Å; Cu−Br = 2.3621(14), 2.3567(13) Å) are slightly shorter when compared to the Cu^{II}(bpy)Br_2 analogue (Cu−N = 2.033(3) Å, Cu−Br = 2.4224(7) Å). The overall geometry of the Cu^{II}(bpy)Br_2 complex is 4 + 2 octahedral because of the long, semicoordinate Cu−Br (3.137 Å) bonds on the adjacent repeat units. This geometry is common in Cu^{II}/halide complexes with $Cu^{II}N_2X_2$ chromophores (X = Br or Cl).[21] In Cu^{II}(dNbpy)Br_2, however, the shortest distance between the Cu atom and the Br atom that does not belong to the same molecule is approximately 5.8 Å, which rules out the possibility of formation of semicoordinate bonds. One reason for this is the steric hindrance imposed on the complex by the long alkyl chains of the dNbpy ligand, which are aligned perpendicularly to the bipyridine planes (Figure 2). This structural modification of the bpy ligand could also be responsible for the unusual 1:1 complex between $Cu^{II}Br_2$ and dNbpy because of a weakening of the binding constant of dNbpy to $Cu^{II}Br_2$, as will be discussed in the next section.

Structure of Cu^{II}(dNbpy)Br_2 in Solution. The Cu^{II}(dNbpy)Br_2 complex, which was isolated from the reaction between $Cu^{II}Br_2$ and dNbpy in CH_3CN, might not be the only species present in the solution. Taking into account the possibility that more than one species might coexist in an equilibrium, the complexation between $Cu^{II}Br_2$ and dNbpy was investigated using absorption spectroscopy. The Vis/NIR region is of particular interest because of the d−d transitions that are very sensitive to the geometry of the Cu^{II} center.[22]

The absorption spectra in the Vis/NIR region of Cu^{II}(dNbpy)Br_2 in both the solid state and the solution can be characterized in terms of the absorption bands around 700 and 500 nm (Figure 3). The extinction coefficients in different solvents, including the typical monomers used in ATRP, are given in Table 3. The maximum absorbance around 500 nm ($\epsilon \approx 900$ L mol^{-1} cm^{-1}) is characteristic of a ligand-to-metal charge transfer (LMCT) from a bromine to the Cu^{II} center.[23−25] The presence of this charge-transfer band in the visible region has been reported for several systems with $Cu^{II}N_2Br_2$ chromophores[26−29] and has been assigned to a square planar arrangement around the Cu^{II} center.[30,31] This is consistent with the solid-state X-ray structure of the Cu^{II}(dNbpy)Br_2 complex. It is still not fully clear why the intensity of this LMCT band is relatively low, but some explanation has been given in which this band can be formally

(19) Garland, M. T.; Grandjean, D.; Spodine, E.; Atria, A. M.; Manzur, J. *Acta Crystallogr., Sect. C*: *Cryst. Struct. Commun.* **1988**, *C44*, 1209−1212.
(20) Hammond, R. P.; Cavaluzzi, M.; Haushalter, R. C.; Zubieta, J. A. *Inorg. Chem.* **1999**, *38*, 1288−1292.
(21) Willet, R. D. *Chem. Coord. Rev.* **1991**, *109*, 181−205.
(22) Wilkinson, G. *Comprehensive Coordination Chemistry*; Pergamon Press: New York, 1987; Vol. 5, pp 674−679.
(23) Ferguson, J. *Prog. Inorg. Chem.* **1970**, *12*, 159−293.
(24) Hush, N. S.; Hobbs, R. J. M. *Prog. Inorg. Chem.* **1968**, *10*, 259−486.
(25) Solomon, E. J.; Penfield, K. W.; Wilcox, D. E. *Struct. Bonding (Berlin)* **1983**, *53*, 1−57.
(26) Ahuja, I. S.; Tripathi, S. *Spectrochim. Acta* **1992**, *48A*, 759−764.
(27) Brierley, M.; Geary, W. J. *J. Chem. Soc. A* **1967**, 963−968.
(28) Brierley, M.; Geary, W. J. *J. Chem. Soc. A* **1968**, 1641−1645.
(29) Ray, N.; Tyagi, S.; Hathaway, B. *J. Chem. Soc., Dalton Trans.* **1982**, 143−146.
(30) Billing, D. E.; Underhill, A. E.; Adams, D. M.; Morris, D. M. *J. Chem. Soc. A* **1966**, 902−907.
(31) Geary, W. J. *J. Chem. Soc. A* **1969**, 71−74.

described as a forbidden or weakly allowed charge transfer from π-bonding orbitals on the bromine to the copper ($2\pi p \rightarrow d\sigma^*$ transition).[32] Recognition of this kind of transition further demonstrated the importance of the π-bonding of the halogen ligands in square planar and tetrahedral Cu^{II} complexes.[33] The maximum absorbance near 700 nm ($\epsilon \approx 230$ L mol^{-1} cm^{-1}) corresponds to the d−d transition. It is characteristic of tetrahedral and square planar Cu^{II} complexes.[34] The similarity of the absorption spectra in the solid state and solution suggests that the geometry of the complex remains unchanged upon dissolution. However, from both Figure 3 and Table 3, it is apparent that the absorption maxima around 500 nm is solvent-dependent. When compared with the solid state, a blue shift is observed in the polar medium, and a red shift is observed in the nonpolar medium. The shift of λ_{max} can also be related to the dielectric constant of the solvent. Generally, for the solvents investigated in this study, the higher the dielectric constant of the solvent is,[35] the lower the λ_{max} for the LMCT band. This phenomenon has previously been observed for a variety of transition metal complexes[36−40] and can be explained in terms of energy localization on bromine ligands. In a polar medium, the Cu−Br bond lengths are more elongated, the electrons are more localized around bromine, and thus, a higher energy (lower λ_{max}) is required for the LMCT transition. On the other hand, in a nonpolar medium, the Cu−Br bond lengths are shorter, the electrons around bromine are more delocalized, and consequently, the LMCT transition occurs at a lower energy (higher λ_{max}).

We have studied the complexation of $Cu^{II}Br_2$ with dNbpy previously using extended X-ray absorption fine structure (EXAFS)[41] and electrospray ionization mass spectrometry (ESI-MS).[42] The EXAFS experiments determined the average Cu−N bond length of 2.040 Å and the average Cu−Br bond length of 2.370 Å. These results are consistent with the bond lengths for Cu^{II}(dNbpy)Br_2 reported in this paper. However, the coordination numbers of nitrogen and bromine were determined to be 4.4 and 3.6, respectively. Taking into account the 20% inherent error in calculating the coordination numbers, the values are still inconsistent with the crystal structure of Cu^{II}(dNbpy)Br_2. However, the EXAFS experiments were performed in methyl acrylate at room temperature using 2 equiv of dNbpy relative to $Cu^{II}Br_2$. Different species can form in solution with higher ratios of dNbpy, as will be discussed in the next section. Recent experiments conducted at Stanford Synchrotron Radiation Laboratory (SSRL)[43] with 1 equiv of dNbpy determined that the Cu^{II} center is coordinated on average by 2.8 nitrogen atoms at the distance of 2.04 Å and 1.7 bromine atoms at the distance of 2.38 Å, which is in better agreement with the crystal structure of Cu^{II}(dNbpy)Br_2.

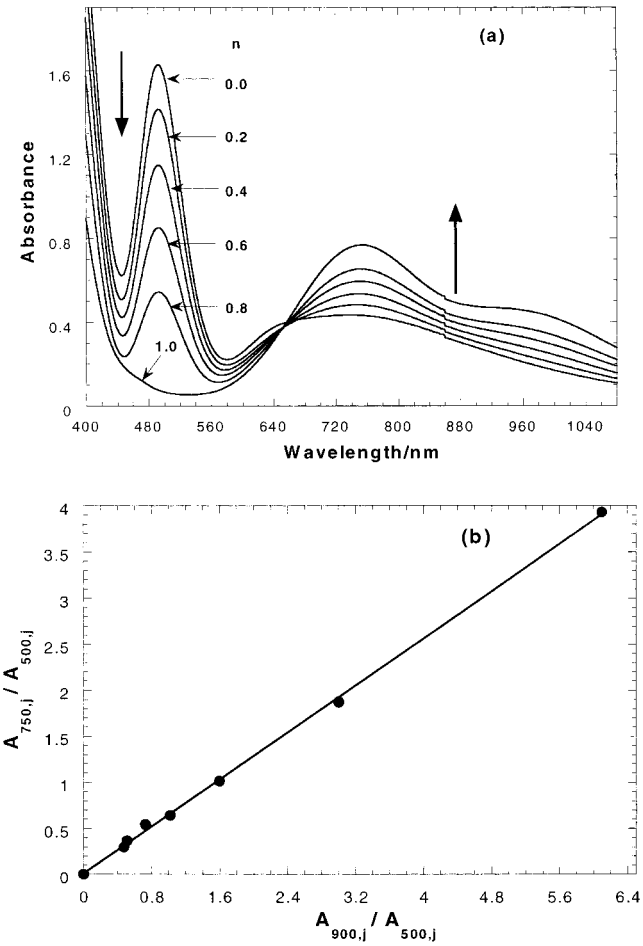

Figure 4. (a) Addition of n equiv of dNbpy to Cu^{II}(dNbpy)Br_2 in CH_3CN at 25 °C. (b) Test for the number of absorbing species in the reaction of Cu^{II}(dNbpy)Br_2 with dNbpy (400−1400 nm). [Cu^{II}(dNbpy)Br_2]$_0 = 1.8 \times 10^{-3}$ M.

The ESI-MS spectra of the $Cu^{II}Br_2$ complex with 1 equiv of dNbpy in a nonpolar medium indicated the presence of $[Cu^{II}(dNbpy)_2Br]^+$ and $[Cu^{II}(dNbpy)Br]^+$ cations and $[Cu^{I}Br_2]^-$ and $[Cu^{II}Br_3]^-$ anions. When 2 equiv of dNbpy was used, an additional peak due to $[Cu^{II}(dNbpy)Br_3]^-$ anions was detected. On the basis of the relative intensities of the different peaks, we concluded that one possible structure of the complex in solution was $[Cu^{II}(dNbpy)_2Br]^+[Cu^{II}Br_3]^-$. This result is inconsistent with the solid-state X-ray structure of Cu^{II}(dNbpy)Br_2. However, if the Cu^{II}(dNbpy)Br_2 complex indeed exists in solution, its intensity would be relatively low in the ESI-MS because of the absence of charge in the complex. This could lead to the wrong conclusion about the most probable structure in solution.

Addition of dNbpy to Cu^{II}(dNbpy)Br_2. As indicated in Figure 4a, the absorption spectrum of Cu^{II}(dNbpy)Br_2 in CH_3CN changes after the addition of dNbpy ligand. The absorbance at 490 nm completely disappears when 1 equiv of dNbpy is added. The disappearance of the 490 nm absorption peak is accompanied by the formation of another absorption peak at 750 nm, with a shoulder centered around 950 nm. The final spectrum in Figure 4a, which does not change on further addition of dNbpy ligand, is typical for a distorted trigonal bipyramidal $[CuN_4X]^+$ chromophore.[44] The splitting pattern of the absorption band represents the deviation from the regular trigonal bipyra-

(32) Crutchley, R. J.; Hynes, R.; Gabe, E. J. *Inorg. Chem.* **1990**, *29*, 4921−4928.
(33) Braterman, P. S. *Inorg. Chem.* **1963**, *2*, 448−452.
(34) Hathaway, B. J.; Billing, D. E. *Coord. Chem. Rev.* **1970**, *5*, 143−207.
(35) Lide, D. R. *Handbook of Organic Solvents*; CRS Press: Boca Raton, FL, 1995.
(36) Perkampus, H. H. *UV−Vis Spectroscopy and Its Applications*; Springer-Verlag: Berlin and Heidelberg, 1992.
(37) Drago, R. S. *Physical Methods for Chemists*, 2nd ed.; Saunders College Publications: Fort Worth, TX, 1992.
(38) Balzani, V.; Carassity, V. *Photochemistry of Coordination Compounds*; Academic Press: New York, 1970.
(39) Wilkinson, G. *Comprehensive Coordination Chemistry*; Pergamon Press: New York, 1987; Vol. 1, Chapter 7.3.
(40) Weit, S. K.; Ferraudi, G.; Grutsch, P. A.; Kutal, C. *Coord. Chem. Rev.* **1993**, *128*, 225−243.
(41) Kickelbick, G.; Reinohl, U.; Ertel, T. S.; Weber, A.; Bertagnolli, H.; Matyjaszewski, K. *Inorg. Chem.* **2001**, *40*, 6−8.
(42) Pintauer, T.; Jasieczek, C. B.; Matyjaszewski, K. *J. Mass. Spectrom.* **2000**, *35*, 1295−1299.
(43) Pintauer, T.; Reinohl, U.; Feth, M.; Bertagnolli, U.; Matyjaszewski, K. Unpublished results.

Scheme 2. Proposed Equilibrium for the Reaction between $Cu^{II}(dNbpy)Br_2$ and dNbpy

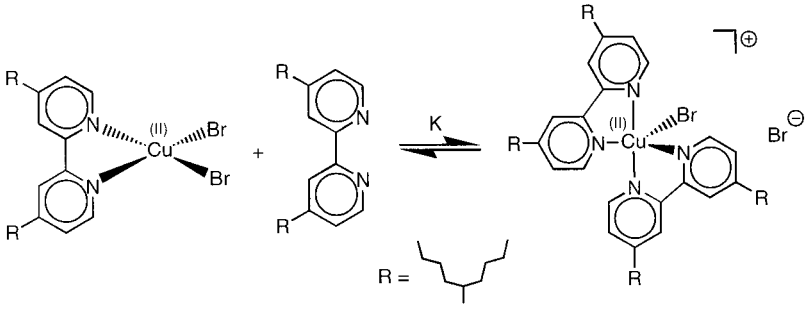

midal geometry. The maximum observed at 750 nm ($\epsilon \approx 350$ L mol^{-1} cm^{-1}), based on the initial concentration of $Cu^{II}(dNbpy)Br_2$), is attributed to the $d_{xy} \approx d_{yz} \rightarrow d_{z^2}$ transition, and the low-energy shoulder at 950 nm ($\epsilon \approx 220$ L mol^{-1} cm^{-1}) is assigned to the $d_{x^2-y^2} \rightarrow d_{z^2}$ transition. The intensity of these bands is affected by the counterion because of the trigonal bipyramidal distortion in $[Cu^{II}(bpy)_2X][Y]$ complexes (X = Br or Cl, Y = PF_6, CF_3SO_3, ClO_4, etc.), as studied using solid-state X-ray crystallography.[17]

To further confirm that the final spectrum in Figure 4a is indeed due to the presence of $[Cu^{II}(dNbpy)_2Br]^+$ cations, three model complexes were prepared with the formula $[Cu^{II}(dNbpy)_2Br][Y]$ (where Y = Br, PF_6, and CF_3SO_3). Data for their solution spectra in different solvents are given in Table 3. All three complexes, including the final spectrum in Figure 4a, have nearly identical absorption spectra; it is therefore apparent that dNbpy reacts with $Cu^{II}(dNbpy)Br_2$ to form the $[Cu^{II}(dNbpy)_2Br]^+[Br]^-$ complex. This clear conversion between the two complexes is indicated in Figure 4a by the isosbestic point at 658 nm. Furthermore, a test for the number of absorbing species by the method of Coleman et al.[45] (Figure 4b) indicates that there are only two species present in the 400−1400 nm region. On the basis of the assumption that the structure of $Cu^{II}(dNbpy)Br_2$ does not change in solution, we propose the equilibrium explaining the effect of dNbpy (Scheme 2).

As indicated in Scheme 2, dNbpy displaces the Br ligand in the neutral $Cu^{II}(dNbpy)Br_2$ complex, and the $[Cu^{II}(dNbpy)_2Br]^+$ cation and $[Br]^-$ anion are formed. This change from a neutral to an ionic species should be accompanied by an increase in the conductivity. Figure 5 shows the plot of conductivity versus the number of equivalents of dNbpy relative to $Cu^{II}(dNbpy)Br_2$ in CH_3CN at 25 °C. The starting solution shows only a residual conductivity of about 1 μS. Addition of the free dNbpy ligand results in an increase in the conductivity, and a plateau is reached at about 1 equiv of added dNbpy. This is consistent with the absorption spectra in Figure 4a and further supports the equilibrium proposed in Scheme 2. The curvature in the conductivity indicates the potential ion pairing between $[Cu^{II}(dNbpy)_2Br]^+$ and $[Br]^-$.[46,47] The value of the equilibrium constant in Scheme 2 in CH_3CN must be relatively large since only 1 equiv of dNbpy is needed to completely shift the equilibrium to the right side. The coordination of the bpy and Br^- ligand to $Cu^{II}Br_2$ in DMF at room temperature has been investigated previously.[48] From the binding constants that were

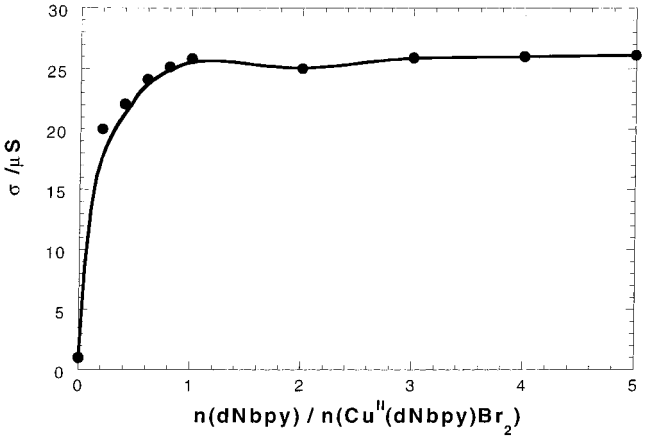

Figure 5. Plot of conductivity vs number of equivalents of dNbpy relative to $Cu^{II}(dNbpy)Br_2$ in CH_3CN at 25 °C, $[Cu^{II}(dNbpy)Br_2]_0 = 2.0 \times 10^{-3}$ M.

determined using calorimetry, it can be estimated that K in Scheme 2 for the bpy ligand in DMF is on the order of 1.0×10^5 L mol^{-1}. A similar value is expected in CH_3CN.

In a less polar medium, such as the monomers that are typically used in ATRP, the equilibrium constant in Scheme 2 is much smaller than in CH_3CN. As indicated in Figure 6a, a higher ratio of dNbpy relative to $Cu^{II}(dNbpy)Br_2$ is needed to shift the equilibrium toward the pentacoordinated $[Cu^{II}(dNbpy)_2Br]^+[Br]^-$ complex. Clearly, the ionic $[Cu^{II}(dNbpy)_2Br]^+[Br]^-$ complex is not favored in the nonpolar medium, and the equilibrium lies preferentially on the side of the neutral $Cu^{II}(dNbpy)Br_2$. This difference in polar and nonpolar mediums enabled us to reverse the equilibrium as indicated in Figure 6b. A distorted trigonal bipyramidal $[Cu^{II}(dNbpy)_2Br]^+[CF_3SO_3]^-$ complex was dissolved in methyl methacrylate, and the changes in the spectra were recorded with the addition of a Br^- source from hexadecyltributylphosphonium bromide (HDTBPBr). In the $[Cu^{II}(dNbpy)_2Br]^+[CF_3SO_3]^-$ complex, the $CF_3SO_3^-$ anion is noncoordinating, as indicated by the solid-state X-ray structure of a related $[Cu^{II}(bpy)_2Br]^+[CF_3SO_3]^-$ compound.[17] When dissolved in methyl methacrylate, the complex displays an absorption spectrum that is consistent with the distorted trigonal bipyramidal $[Cu^{II}(dNbpy)_2Br]^+$ cation. The absorbance at 520 nm increases as the amount of HDTBPBr increases, and no further changes in the spectrum are observed at ratios higher than 2 equiv of HDTBPBr. The equilibrium was completely shifted toward the $Cu^{II}(dNbpy)Br_2$ complex.

To confirm that dNbpy was released in the reaction (the reverse of the equilibrium in Scheme 2), a qualitative experiment was performed. A solution obtained by mixing the $[Cu^{II}(dNbpy)_2Br]^+[CF_3SO_3]^-$ complex with 2 equiv of HDTBPBr in methyl methacrylate was run through an alumina column to

(44) Murphy, G.; O'Sullivan, C.; Murphy, B.; Hathaway, B. *Inorg. Chem.* **1998**, *37*, 240−248.
(45) Coleman, J. S.; Varga, L. P.; Mastin, S. H. *Inorg. Chem.* **1970**, *9*, 1015−1020.
(46) Grattan, D. W.; Plesch, P. H. *J. Electroanal. Chem.* **1979**, *103*, 81.
(47) Holdcroft, G. E.; Plesch, P. H. *J. Chem. Res. Synop.* **1985**, *36*.
(48) Ishiguro, S.; Nagy, L.; Ohtaki, H. *Bull. Chem. Soc. Jpn.* **1987**, *60*, 2053−2058.

Table 4. Thermodynamic Data for Equilibrium in Scheme 2 in Different Solvents

solvent	dielectric constant (ϵ)	K_{298} (L mol^{-1})[a]	K_{363} (L mol^{-1})[a]	$\Delta H°$ (kJ mol^{-1})[b]	$\Delta S°$ (J K^{-1} mol^{-1})[b]
toluene	2.38[20]	13.4 ± 0.54	0.810 ± 0.032	−39.2 ± 3.4	−110 ± 5.6
styrene	2.47[20]	15.5 ± 0.93	1.13 ± 0.068	−36.0 ± 2.3	−98.1 ± 7.6
n-BA	5.63[20]	78.0 ± 3.1	6.93 ± 0.27	−33.7 ± 3.1	−76.7 ± 6.9
MMA	6.32[30]	72.0 ± 2.9	2.02 ± 0.081	−49.4 ± 3.1	−130 ± 7.4
MA	7.03[30]	251 ± 12.6	0.847 ± 0.042	−78.7 ± 3.9	−218 ± 11

[a] Single experiment, analysis performed at 500, λ_{max} near 500 (see Table 3) and 540 nm. [b] Thermodynamic parameters calculated from van't Hoff plot at five different temperatures.

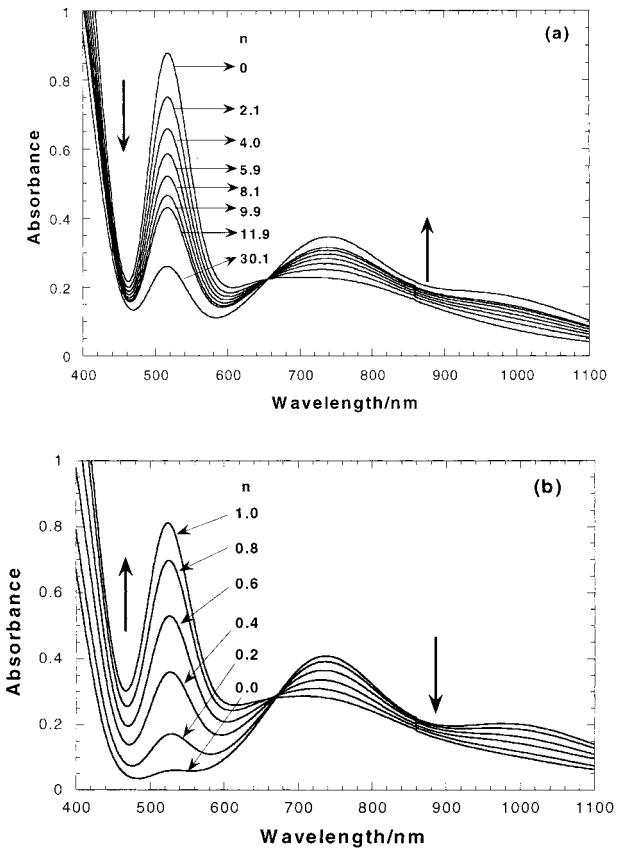

Figure 6. (a) Addition of *n* equivalents of dNbpy to Cu^{II}(dNbpy)Br_2 in MMA at 25 °C, $[Cu^{II}(dNbpy)Br_2]_0 = 1.0 \times 10^{-3}$ M. (b) Addition of *n* equivalents of HDTBPBr to $[Cu^{II}(dNbpy)_2Br][CF_3SO_3]$ in MMA at 25 °C, $\{[Cu^{II}(dNbpy)_2Br][CF_3SO_3]\}_0 = 1.1 \times 10^{-3}$ M.

remove the Cu^{II} complex. The clear solution was evaporated, and the residue was dissolved in C_6D_6. ^{1}H NMR analysis indicated the presence of dNbpy. When the pure Cu^{II}(dNbpy)Br_2 complex in methyl methacrylate was passed through an alumina column, dNbpy could not be detected, which indicated that dNbpy was released from the $[Cu^{II}(dNbpy)_2Br]^+[CF_3SO_3]^-$ complex.

Determination of the Equilibrium Constant. The equilibrium constant for the reaction between dNbpy and Cu^{II}(dNbpy)Br_2 (Scheme 2) in nonpolar medium can be determined using the method of Drago.[49] Initially, the solution contains the Cu^{II}(dNbpy)Br_2 complex (c_0) and *n* equiv of dNbpy ligand (nc_0). At equilibrium, $[Cu^{II}(dNbpy)Br_2] = c_0(1 - x)$, $[dNbpy] = c_0(n - x)$, and $[Cu^{II}(dNbpy)_2Br]^+[Br]^- = c_0x$, where $x = (A_0 - A_{EQ})/(A_0 - A_\infty)$ (A_0 = initial absorbance of Cu^{II}(dNbpy)Br_2 at λ_{max}, A_{EQ} = absorbance at the equilibrium position, A_∞ = absorbance when the equilibrium in Scheme 2 is totally shifted toward its right-hand side). The equilibrium constant *K* can then be expressed as

$$K = \frac{x}{c_0(1 - x)(n - x)}$$

or

$$\frac{Kc_0}{x} = \frac{1}{(1 - x)(n - x)}$$

The plot of $1/(1 - x)(n - x)$ versus $1/x$ is a straight line passing through the origin (Supporting Information). The equilibrium constant *K* can then be determined from the slope of the regression line and the initial concentration of Cu^{II}(dNbpy)Br_2 (slope = Kc_0). The *K* values correspond to the apparent equilibrium constant, which is related to the absolute value described in Scheme 2 and the dissociation constant of the resulting ion pairs to the free ions. It seems that the latter must be quite small, since even the most polar acetonitrile conductivity measurements indicate significant ion pairing. $\Delta H°$ and $\Delta S°$ can be calculated from variable temperature studies (Supporting Information). The thermodynamic data for different monomers used in ATRP and in toluene are summarized in Table 4. The *K* values at 25 and 90 °C are included for comparison. The equilibrium constant at room temperature increases as the dielectric constant of the medium increases. The reaction is exothermic in all solvents, as indicated by the negative $\Delta H°$ values. Similarly, $\Delta S°$ values are also negative. The reaction becomes less favored as the temperature increases, and the Cu^{II}(dNbpy)Br_2 complex is more favored. From Table 4, $\Delta H°$ is also related to the dielectric constant of the medium. Generally, $\Delta H°$ decreases as the dielectric constant increases, and the reaction becomes more exothermic. This can be explained in terms of lowering the relative energy of the ionic product and/or alternatively raising the energy of the reactants. The polar medium favors the formation of the $[Cu^{II}(dNbpy)_2Br]^+[Br]^-$ complex because the charges on the $[Cu^{II}(dNbpy)_2Br]^+$ cation and the $[Br]^-$ anion can be stabilized. The nonpolar medium, on the other hand, favors the formation of the neutral Cu^{II}(dNbpy)Br_2 complex. The entropy values in toluene, styrene, *n*-butyl acrylate, and methyl methacrylate are in the range of -110 ± 26 J K^{-1} mol^{-1}, which corresponds to the loss of three degrees of translational entropy because of the immobilization of the dNbpy molecule. More negative entropy for the most polar methyl acrylate indicates additional solvation of the polar ionic complex. Without knowledge of the individual rate constants for this equilibrium, it is difficult to draw any conclusions regarding the mechanism for this ligand substitution. In the dissociative case, the transition state is expected to consist of $[Cu^{II}(dNbpy)Br]^+$ and $[Br]^-$. On the other hand, if the reaction proceeds via an associative mechanism, the transition state would resemble a neutral octahedral $[Cu^{II}(dNbpy)_2Br_2]$ complex.

In a typical reverse ATRP of styrene at 110 °C, the starting Cu^{II} complex was prepared by mixing $Cu^{II}Br_2$ with 2 equiv of

(49) Beugelsdijk, T. J.; Drago, R. S. *J. Am. Chem. Soc.* **1975**, *97*, 6466−6473.

the dNbpy ligand. The initial concentration of the Cu^{II} complex was approximately 1.0×10^{-1} M.[12] According to the equilibrium in Scheme 2, both $Cu^{II}(dNbpy)Br_2$ and $[Cu^{II}(dNbpy)_2Br][Br]$ are expected to form under these conditions. The equilibrium constant of 0.61 L mol^{-1} at 110 °C can be calculated from the data in Table 4, and it implies that initially the styrene solution contains approximately 95% of the neutral $Cu^{II}(dNbpy)Br_2$ complex and 5% of the ionic $[Cu^{II}(dNbpy)_2Br]^+[Br]^-$. This nearly 1:1 stoichiometry between $Cu^{II}Br_2$ and dNbpy is also an indication of the presence of free dNbpy ligand in the system. Under the same conditions, the neutral $Cu^{II}(dNbpy)Br_2$ is also dominant in other monomers.

Both complexes are expected to be active in the deactivation process shown in Scheme 1. The subject of further investigation is to determine which of the two shows a higher activity toward reduction by the $R^\bullet$ radical and to determine what is the structure of the corresponding Cu^I complex. The correlation between Cu^I and Cu^{II} structures in conventional and reverse ATRP, together with the role of free dNbpy ligand in these systems, will also be considered.

Conclusion

The solid-state X-ray structure of a novel compound $Cu^{II}(dNbpy)Br_2$ was reported. The Cu^{II} center in this complex, which is used as the catalyst for the reverse ATRP, has a distorted square planar geometry and is coordinated by the nitrogen atoms of a single dNbpy ligand and two bromine atoms. The average Cu−N and Cu−Br bond lengths were determined to be 2.017 and 2.359 Å, respectively. In the presence of dNbpy ligand, this complex undergoes Br substitution to form ionic $[Cu^{II}(dNbpy)_2Br]^+[Br]^-$. $\Delta H°$ and $\Delta S°$ for this equilibrium were negative and dependent on the dielectric constant of the medium. It was found that under the typical polymerization conditions ($T \geq 90$ °C and the total copper concentration in the range 1.0×10^{-2}−1.0×10^{-1} M), $Cu^{II}Br_2$ and 2 equiv of dNbpy predominantly formed the neutral $Cu^{II}(dNbpy)Br_2$ complex. In polar medium, $[Cu^{II}(dNbpy)_2Br]^+[Br]^-$ was preferred. The activity of these two complexes in reverse ATRP and the possibility for the presence of $Cu^{II}(dNbpy)Br_2$ in conventional ATRP are currently under investigation.

Acknowledgment. The authors acknowledge Kelly Davis for providing the dNbpy ligand. The financial support from the the National Science Foundation, the U.S. Environmental Protection Agency, and the Fonds zur Förderung der wissenschaftlichen Forschung-Vienna is greatly appreciated.

Supporting Information Available: X-ray crystallographic file for $Cu^{II}(dNbpy)Br_2$ (in CIF format), determination of the equilibrium constant, and thermodynamic parameters for bromine substitution by dNbpy in $Cu^{II}(dNbpy)Br_2$. This material is available free of charge via the Internet at http://pubs.acs.org.

IC0100267